Effect of methane concentration on reaction behavior in direct-methane solid oxide fuel cells with $(Ce,Gd)O_{2-x}$-impregnated FeCr layer for fuel processing

Ta-Jen Huang*, Meng-Chin Huang

Department of Chemical Engineering, National Tsing Hua University, 101 Kuang Fu Road, Sec. 2, Hsinchu 300, Taiwan, ROC

ABSTRACT

A solid oxide fuel cell (SOFC) with a Ni-yttria-stabilized zirconia anode of $1\,cm^2$ area was set up with a porous disk of gadolinia-doped ceria-impregnated FeCr as a gas diffusion layer (GDL) under direct-methane feeding. In this setup of SOFC plus GDL, the tests at $800\,°C$ and ambient pressure show that the current density, the methane conversion rate, the product formation rates, and the CO_2 selectivity increased with increasing methane concentration. The major reaction in the GDL is CO_2 reforming of methane to produce the syngas (CO plus H_2). The anodic electrochemical oxidation of CO from GDL results in an overall rate of CO_2 formation being much larger than that of CO formation. There is a synergy between the rate of reaction in the GDL and that over the anode.

© 2009 Elsevier B.V. All rights reserved.

1. Introduction

Methane is an attractive fuel for solid oxide fuel cells (SOFCs). A great deal of research efforts have been put on the conversion of methane fuel into hydrogen-rich gas as required for the electrochemical reaction on the anode. Recently, SOFCs with internal reforming, either direct or indirect internal reforming [1–3], have attracted much attention since the requirement for a separate fuel reformer can thus be eliminated and the efficiency is increased by effective utilization of waste heat. Depending on the operating conditions, the heat consumed by internal reforming can vary from 40 to 70% of the total heat produced in a fuel cell [1]. Therefore, internal reforming SOFC is an energy efficient system design. However, over the usual Ni anode, coking is a well-known problem when methane is used as the fuel. Although the coking problem may be overcome by adding enough steam into the fuel stream, fuel dilution becomes a problem [1], in addition to the extra heating energy required to produce the steam. Direct-methane SOFCs (DM-SOFCs) with either an inert porous layer [4] or a catalyst layer [5] placed between the anode and the fuel stream are promising to solve the coking problem.

Methane decomposition occurs over the Ni anode in DM-SOFCs [6,7]. At high temperatures, methane may decompose to produce the C species, the reaction being $CH_4 \rightarrow C + 2H_2$, similar to thermal cracking of methane. The deposited C species over Ni may cause coking [8], which can cause very rapid deactivation of the SOFC anode; consequently, the removal of the deposited carbon should be important. However, a carbon SOFC has been proposed to utilize the deposited carbon as a fuel [9]. Huang and Huang [10] have confirmed that the deposited carbon can be fully utilized for the generation of the electrical current.

FeCr alloy can be used as the interconnect materials for intermediate temperature SOFCs [11]. Thus, FeCr can be utilized as the current collector over the SOFC anode. A porous FeCr disk has been used as the gas diffusion layer (GDL) and also as the current collector over the anode side of a DM-SOFC to achieve a stable SOFC performance [12]. Additionally, the surface of the FeCr disk has been modified by adding powders of yttria-stabilized zirconia (YSZ) and Ni-YSZ, which results in a better DM-SOFC performance than the FeCr disk without surface modification [12].

The FeCr GDL can function as a catalyst layer for fuel processing in DM-SOFCs [12]. In SOFCs, a catalyst layer for fuel processing has been studied and enhanced performance has been observed [5,13–16]. However, the reaction behavior in this catalyst layer has seldom been studied. For the design of the catalyst layer for fuel processing in SOFCs, the clarification of the reaction behavior in this catalyst layer should be useful.

The Ni anode with a coating of doped ceria has been used for direct utilization of methane in low-temperature SOFCs [17]; the coating of Sm-doped ceria with the impregnating method to a porous Ni anode layer enhances the anode performance. Huang and Huang [18] have reported that the impregnation of

* Corresponding author. Tel.: +886 3 5716260; fax: +886 3 5715408.
E-mail address: tjhuang@che.nthu.edu.tw (T.-J. Huang).

gadolinia-doped ceria (GDC) onto the surface of the porous FeCr GDL results in a relatively stable DM-SOFC performance.

In the work, GDC was added by impregnation to the surface of a porous FeCr disk, which was used as the GDL and also as the current collector over the anode of DM-SOFCs. The anode had an area of $1 \, cm^2$. Anode fuels with various methane concentrations were used. In this setup of SOFC plus GDL, the tests at 800 °C and ambient pressure show that the overall rate of CO_2 formation is larger than that of CO formation. The major reaction in the GDL is shown to be CO_2 reforming of methane to produce the syngas (CO plus H_2). There is a synergy between the rate of reaction in the GDL and that over the anode.

2. Experimental

2.1. Preparation of GDC-impregnated FeCr disk

GDC powder was prepared by a co-precipitation method. The details of the method have been reported elsewhere [19]. The calcinations of the GDC powders were carried out by heating in air at a rate of 10 °C/min to 300 °C and held for 2 h, and then to 700 °C and held for 4 h, and then slowly cooled down to room temperature. GDC of this work is $(GdO_{1.5})_{0.1}(CeO_2)_{0.9}$.

Porous FeCr disk was prepared by mixing FeCr powder (Goodfellow, Fe 87.5% and Cr 12.5%, particle size 45 μm) and graphite powder (Aldrich, synthetic, particle size <20 μm) in a weight ratio of graphite:FeCr = 3:4. 0.5 g of the mixture powders was compressed with 10 ton into a disk. Then, the disk was calcined at 1200 °C to make it porous. The FeCr disk has a porosity of 78%, an area of $1 \, cm^2$ and a thickness of 0.22 cm.

The addition of GDC onto the FeCr disk was done by impregnation. The porous FeCr disk was impregnated with solution of GDC precursor equivalent to 26% GDC with respect to the weight of FeCr. After drying, the disk was heated to 800 °C to form GDC over the surface of the porous FeCr disk. This is a surface modification of the FeCr disk.

2.2. Construction of the SOFC unit

The commercial YSZ tape (156 μm thickness, Jiuhow, Taiwan) was employed to make an electrolyte-supported cell. A disk of 1.25 cm diameter was cut from the tape. One side of the disk was coated with the Ni-YSZ paste, which was made of 60 wt% Ni-YSZ powder, corn oil, polyvinyl butyral, and ethanol. The other side of the disk was screen-printed with a thin layer of Pt paste (Heraeus, C3605P) to make the cathode layer.

The method of the coating of the Ni-YSZ paste to make the anode layer has been described elsewhere [10]. The thus-prepared unit cell has an anode area of $1 \, cm^2$, an anode thickness of about 30 μm, an electrolyte thickness of 156 μm, a cathode area of $1 \, cm^2$ and a cathode thickness of about 5 μm. These thicknesses were measured from a scanning electron micrograph plot of the cross-section of the unit cell.

Completed unit cell was closely connected with the GDC-impregnated FeCr disk on the anode side and Pt mesh on the cathode side, and then with Pt wires to the current and voltage measurement unit. The ceramic paste was used to seal the unit cell in a quartz tube with a heat treatment of 400 °C for 1.5 h so as to complete the preparation of the test unit with a single cell. The anode side of the unit cell is sealed in the quartz tube and the cathode side is exposed to stagnant air.

A sketch of the setup, identifying the different layers of the SOFC unit and their dimensions and showing how the SOFC unit cell is embedded in the quartz tube, has been reported elsewhere [20]. For the measurement of the temperature of the unit cell, the
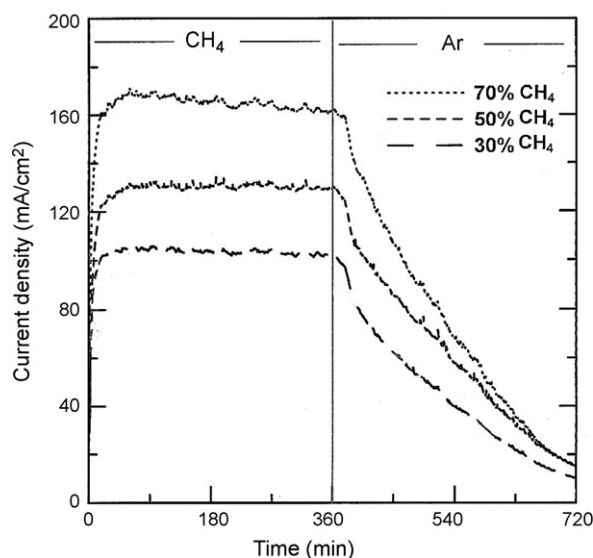

Fig. 1. Variation of the profiles of current density with methane concentration.

thermocouple was placed on the anode side and touched the FeCr disk.

2.3. Activity tests of unit cell

A voltage of 0.61 V was maintained for all tests in this work. The test temperature was fixed at 800 °C. The tests were conducted at ambient pressure. For reduction, the feed to the anode side was 10% H_2 in argon. For the direct-methane test, the fuel to the anode side was 10.5–70% methane (99.9% purity) in argon. The flow rate was always 100 ml/min passing the anode side.

All tests started with the reduction of the anode at 400 °C in 10% H_2 for 1 h. Then, pure argon flow was passed for 2 h to purge the system. The test unit was then heated in argon to 800 °C at a rate of 5 °C/min. Then, the direct-methane test was carried out with introducing methane fuel flow for 360 min. Then, the anode-side flow was switched to argon; the argon flow was kept until the measured electrical current became zero.

During the testing, electrical current, voltage, and outlet gas compositions were continuously measured. The concentrations of CO and CO_2 were measured by CO-NDIR and CO_2-NDIR (non-dispersive infrared analyzer, Beckman 880), respectively. Other gas compositions were measured by two gas chromatographs (China Chromatography 8900) in series.

The gas chromatographs (GCs) were equipped with molecular sieve 5A column (GC1) and Porapak Q column (GC2), respectively. GC1 was used to measure the concentration of water in the product stream; a molecular sieve 5A column was placed in between GC1 and GC2 to remove possible content of water; GC2 was used to measure the concentrations of hydrogen and methane. Thermal conductivity detector was used for both GCs. The GC carrier gas was argon with 99.9995% purity. GC measurements were carried out every 10 min with auto-sampling. GC calibrations were carried out or checked before each test.

3. Results and discussion

3.1. Variation of current density with methane concentration

Fig. 1 shows the variation of the profiles of the current density with the methane concentration. The current density increases as the methane concentration increases from 30 to 70% CH_4, as also shown in Table 1. A steady-state or stable current density can be

Table 1
Effects of methane concentration on averaged[a] current density, methane conversion rate, product formation rates and CO_2 selectivity.

% CH_4	Current density (mA/cm^2)	ΔCH_4[b]	H_2[c]	CO_2[c]	CO[c]	CO_2 selectivity[d]
30	103.2	26.5	53.0	20.03	7.70	0.722
50	130.5	31.0	62.0	23.60	8.74	0.730
70	164.1	45.2	90.5	34.98	12.11	0.743

[a] The averaged value of the data taken during the SOFC operation from 200 to 300 min.
[b] Methane conversion rate in $\mu mol/cm^2$ min.
[c] Formation rate in $\mu mol/cm^2$ min.
[d] Defined as $CO_2/(CO + CO_2)$.

obtained; this indicates that the amount of the deposited C species over the anode was small and thus possible coking was not serious to result in a deactivation of the performance of the direct-methane SOFCs. This is attributed to the existence of the FeCr GDL, which processed the methane fuel so as to reduce its concentration of reaching the anode; thus, carbon formation over the anode can be reduced so as not to deactivate the SOFC performance.

Fig. 1 also shows that, when the anode-side flow is switched to argon, an electrical current is measured continuously for a period longer than that of CH_4 flow. Notably, the anode compartment can be purged to become methane free in less than 2 min after switching to Ar flow. Additionally, during Ar flow, the current density is larger if the methane concentration during CH_4 flow is larger, noting that the same SOFC unit cell was used. This indicates the electrochemical oxidation of the C species which was deposited during CH_4 flow via methane decomposition, noting that a larger methane concentration during CH_4 flow can result in a larger amount of the deposited C species. Therefore, although the electrochemical oxidation of the Ni metal which may be formed during CH_4 flow may also occur, the electrochemical oxidation of the deposited C species should be the major reaction during the initial period of Ar flow. Notably, the generation of an electrical current via the electrochemical oxidation of the deposited C species during Ar flow is similar to that of a carbon SOFC [9]. Additionally, during the latter period of argon flow, a fuel-free current can occur due to a deficiency of the bulk lattice-oxygen concentration on the anode side during methane flow, which results from the electrochemical promotion of bulk lattice-oxygen extraction [10].

3.2. Variation of product formation rates and CH_4 conversion rate

Fig. 2 shows the product formation rates and CH_4 conversion rate with 30% CH_4 as the fuel. Since there is no H_2O formation, the major CH_4 reaction during these DM-SOFC operations should be the dissociation of methane without hydrogen oxidation. Notably, no H_2O formation is claimed only to indicate that no H_2O vapor can be detected within the detection limit of the gas chromatograph used in this work. Table 1 shows that the amount of hydrogen formed is two times that of methane converted; this indicates that the hydrogen constituent of methane has been completely converted to hydrogen gas and thus no H_2O would have been formed. Notably, also, DM-SOFC operation without H_2O formation has been observed previously either in an SOFC with GDL [12] or in one without GDL [10]; this is attributed to stronger interaction of the C species with the catalyst surface than that of hydrogen; restated, hydrogen cannot compete with the C species to be adsorbed onto the anode Ni surface [12]. This behavior of no H_2O formation either over the anode or in the GDL indicates the inertness of the SOFC towards H_2 conversion during direct-methane reaction. Additionally, SOFC operation with the coal syngas (CO plus H_2) as the fuel has led to an observation that the reactivity of CO is higher than that of H_2; this is attributed to stronger C-metal interaction than the H-metal
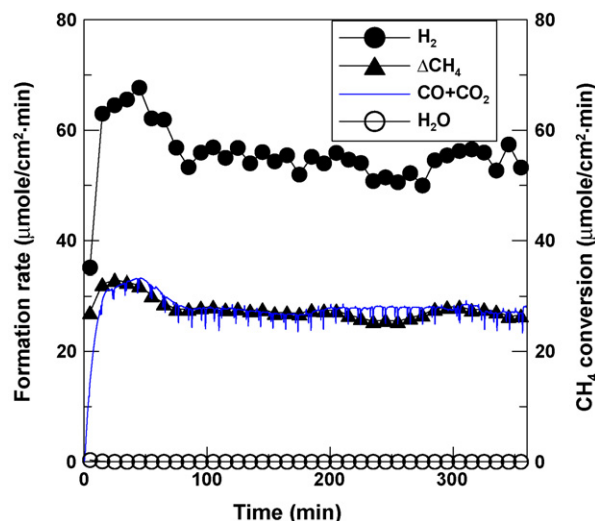

Fig. 2. Profiles of product formation rates and CH_4 conversion rate with 30% CH_4 as the fuel.

interaction [21]. Thus, the observation of no H_2O formation in this work, both in the GDL and over the anode, is attributed to stronger interaction of the C species with the catalyst surface than that of hydrogen. Notably, also, for applications, the SOFC unit cells are assembled to a stack and thus, after the consumption of methane in the upstream SOFC unit cells, the remaining hydrogen can be consumed in the downstream ones, where H_2 conversion to H_2O will not be a problem.

Fig. 2 also shows that the rates go up and down initially. During the initial period of about 40 min, the methane conversion rate is larger than the formation rate of CO_x, i.e., CO plus CO_2. This indicates the deposition of the C species, i.e., $\Delta C \neq 0$:

$$\Delta C = \Delta CH_4 - \Delta(CO + CO_2) \tag{1}$$

where ΔC is the amount of the deposited C species, ΔCH_4 is the rate of methane conversion, and $\Delta(CO + CO_2)$ is the amount of CO plus CO_2. After this initial period, the formation rate of CO_x becomes larger than the methane conversion rate. This indicates the oxidation of the deposited C species, a period of de-coking. Therefore, the initial increase of the rates can be attributed to the deposition of the C species and the followed going down of the rates be attributed to the oxidation of these deposited C species. Notably, the deposited carbon cannot be removed by electrochemical oxidation quickly enough; this is attributed to the fact that some deposited carbon is formed on the top-most surface of the anode [6], whereas electrochemical oxidation proceeds at the triple phase boundary and its rate is larger the closer to the bottom of the anode. This is shown in Fig. 2 that the amount of initially deposited carbon is much larger than that of removed carbon at the latter stage of methane flow. This is also attributed to simultaneous occurrence of carbon deposition and de-coking during the latter stage of methane flow. Therefore, some of the deposited carbon remains and can be electrochemically oxidized to generate an electrical current during argon flow, as shown in Fig. 1.

Fig. 2 also shows that the initial going up and down of the methane conversion rate and the CO_x formation rate is in accordance with the initial behavior of the H_2 formation rate. During the deposition of the C species, H_2 is formed according to

$$CH_4 \rightarrow C + 2H_2 \tag{2}$$

and thus the H_2 formation rate goes up in association with methane conversion. Then, during the oxidation of the deposited C species, there is no H_2 formation and thus the H_2 formation rate goes down.
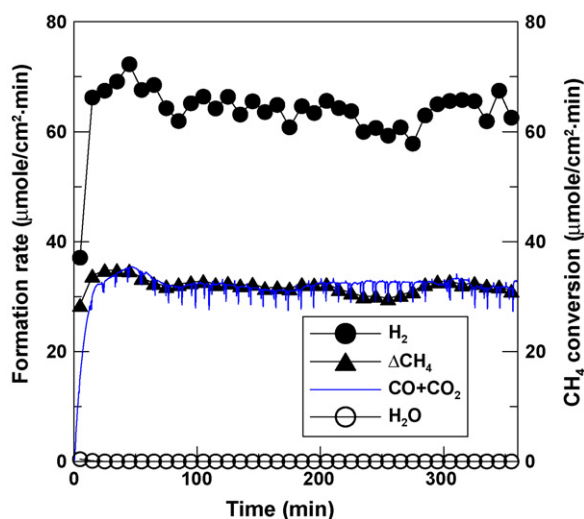
Fig. 3. Profiles of product formation rates and CH_4 conversion rate with 50% CH_4 as the fuel.

After the oxidation of some of the initially deposited C species to free some of the active sites, the methane conversion rate can equal the CO_x formation rate, as shown in Fig. 2 after about 100 min of SOFC operation. In this case, the rate of H_2 formation (ΔH_2) is about two times that of methane conversion (ΔCH_4); Table 1 shows that ΔH_2 is two times ΔCH_4. This is in accordance with the occurrence of the reactions of

$$CH_4 + O \rightarrow CO + 2H_2 \tag{3}$$

and/or

$$CH_4 + 2O \rightarrow CO_2 + 2H_2 \tag{4}$$

in the GDL, where O is the lattice-oxygen species, or with the occurrence of the reactions of

$$CH_4 + O^{2-} \rightarrow CO + 2H_2 + 2e^- \tag{5}$$

and/or

$$CH_4 + 2O^{2-} \rightarrow CO_2 + 2H_2 + 4e^- \tag{6}$$
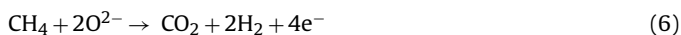
over the anode, where O^{2-} is the oxygen-ion species coming from the cathode. Since the formation of H_2O would decrease the rate of H_2 formation, ΔH_2 being two times ΔCH_4 agrees with the observation of no H_2O formation. Notably, also, there is a period between 200 and 300 min of SOFC operation when the oxidation of the deposited C species occurs to form CO and/or CO_2 and the rate of H_2 formation goes down; this is associated with a decrease of the methane conversion rate, as also shown by $\Delta CH_4 < \Delta(CO + CO_2)$ in Table 1.

Fig. 3 shows the product formation rates and CH_4 conversion rate with 50% CH_4 as the fuel. These rates also go up and down initially as with 30% CH_4. Initially, the rate of methane conversion is also larger than that of CO_x formation, indicating the deposition of the C species. However, this period of C deposition with 50% CH_4 is longer than that with 30% CH_4. This longer period of C deposition is attributed to higher CH_4 concentration.

Fig. 4 shows the product formation rates and the CH_4 conversion rate with 70% CH_4 as the fuel. There is also an initial period of C deposition and this period is again longer than that with 50% CH_4. However, the rates do not go up and down initially as those with 30 and 50% CH_4 as the fuel, but increase continuously until reaching a steady-state. This is attributed to that higher methane concentration leads to larger rate of methane conversion, as shown in Table 1, and thus higher concentration of the C species, according to reaction (2). The C species in the GDL can be oxidized by the

oxygen species extracted from the lattice of GDC in the GDL to form CO and/or CO_2 according to the following de-coking reactions [12]:

$$C + O \rightarrow CO \tag{7}$$

$$C + 2O \rightarrow CO_2 \tag{8}$$

Notably, a combination of reactions (7) and (8) with reaction (2), respectively, results in reactions (3) and (4). Notably, also, electrochemical promotion of bulk lattice-oxygen extraction can occur over the anode of DM-SOFCs with the Ni-YSZ anode [22,23] or the Ni-GDC anode [24]. Since the GDL is functioned as the current collector, there is electrical current passing the GDL and thus electrochemical promotion of bulk lattice-oxygen extraction can also occur in the GDL. Additionally, bulk lattice-oxygen extraction can also occur without electrical current, such as at open circuit [23] or over the GDC catalysts [25–27]. If the concentration of the C species is not high enough, the amount of lattice O species which can be extracted from the GDC bulk in the GDL can be enough to result in a total rate of CO and CO_2 formations to become higher than the steady-state one; this is what happens with methane concentration of 30 or 50% during the initial period as shown in Figs. 2 and 3. However, with the further increase of the methane concentration to 70%, the concentration of the C species becomes so high that the amount of extracted lattice O species cannot results in a total rate of CO and CO_2 formations to become higher than the steady-state one, as shown in Fig. 4. This is attributed to the limitation on the amount of lattice O species which can be extracted [28].

3.3. CO_2 selectivity

Fig. 5 shows that the rate of CO_2 formation is larger than that of CO formation initially. This is attributed to high concentration of surface lattice oxygen over GDC initially, noting that the formation of CO_2 but not CO is favored in the presence of surface lattice oxygen over GDC [27]. Then, the rate of CO_2 formation drops while that of CO formation keeps increasing; this results in a larger rate of CO formation than that of CO_2 formation.

The impregnation of GDC over the FeCr surface results in the formation of the Fe-GDC interface, which can act as the active site for the dissociation of methane and the supply of the O species. Notably, the surface lattice oxygen of GDC alone can act as the active site for the dissociative adsorption of CH_4 [27]. The occurrence of reactions (3) and/or (4) in the GDL consumes the lattice oxygen of GDC. Notably, the consumption of the lattice oxygen generates the
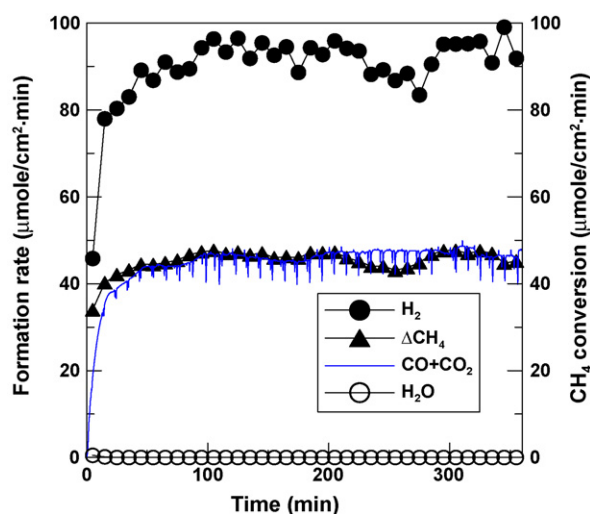

Fig. 4. Profiles of product formation rates and CH_4 conversion rate with 70% CH_4 as the fuel.
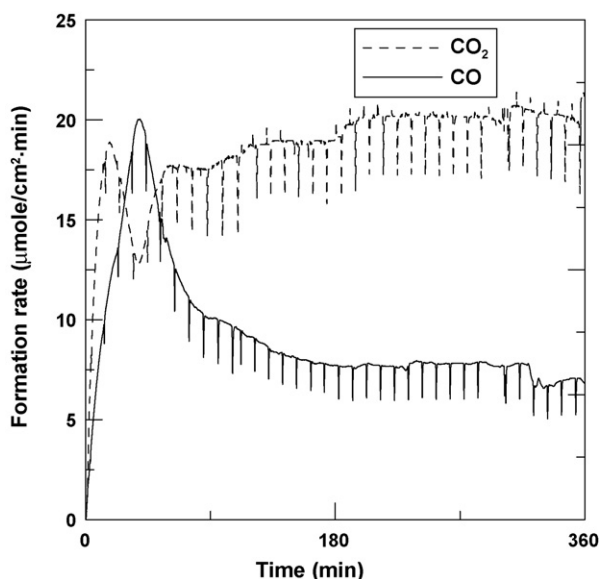
Fig. 5. Profiles of CO and CO_2 formation rates with 30% CH_4 as the fuel.

oxygen vacancy [29]. Then, the transport of CO from the GDL to the anode can induce the electrochemical oxidation of CO over the anode [12]:

$$CO + O^{2-} \rightarrow CO_2 + 2e^- \qquad (9)$$

which enhances the SOFC performance in terms of the current density, in comparison to SOFCs without GDL. In the GDL, the presence of the Fe-GDC interface or GDC active site can lead to the replenishment of the lattice oxygen of GDC by the O species from the dissociation of CO_2 coming from the anode [12]:

$$CO_2 \leftrightharpoons CO + O \qquad (10)$$

This in turn enhances reactions (7) and (8). Notably, the combination of reactions (7) and (10) is CO_2 de-coking [30]:

$$C + CO_2 \leftrightharpoons 2CO \qquad (11)$$

In the GDL, noting that reaction (3) is a combination of reactions (2) and (7), one may combine reactions (2) and (11) to result in an overall reaction of methane with CO_2 coming from the anode:

$$CH_4 + CO_2 \rightarrow 2CO + 2H_2 \qquad (12)$$

which is the reaction of CO_2 reforming of methane [31]. This reaction is the major reaction in the GDL, as will be clarified in the following.

The initial drop of the rate of CO_2 formation is attributed to the concentration of the surface lattice oxygen over GDC being exhausted. Notably, the decrease of the concentration of surface lattice oxygen over GDC is due to that the rate of consumption of the O species for CO_x formation is higher than that of replenishment of the O species via reaction (10). However, this occurs only initially; then, the rates can come to a balance. As shown in Fig. 5, the rate of CO formation reaches a maximum when that of CO_2 formation reaches a minimum; both the maximum and the minimum occur at the same time, about 40 min of SOFC operation, when the initial period of carbon deposition shifts to that of de-coking, as shown by comparing Figs. 2 and 5. Then, the rate of CO_2 formation increases while that of CO formation decreases, leading to larger rate of CO_2 formation than that of CO formation.

Since reaction (12) produces two CO, which may lead to the formation of two CO_2 over the anode, but the replenishment of the lattice oxygen in the GDL via reaction (10) needs only one CO_2, there can be a net rate of the formation of one more CO_2 in the

setup of SOFC plus GDL. This agrees with the observation that the overall rate of the formation of CO_2 is much higher than that of CO, as shown in Table 1. However, in an SOFC without GDL, more CO than CO_2 is produced [12]. Thus, CO_2 reforming of methane to produce the syngas should be the major reaction in the GDL and the GDL of this work should have such a fuel processing capability as to result in the major part of methane conversion occurring in the GDL than over the anode. It is also possible that, over the anode, CO from the GDL competes with that of methane for the active sites so as to reduce the methane conversion.

In the GDL, increasing methane concentration results in an increase of the amount of the deposited C species and thus increases the amount of CO formed. This leads to higher amount of CO_2 formed over the anode and thus the CO_2 selectivity can increase with increasing methane concentration. This is indeed the case as shown in Table 1 and in accordance with the above proposal that the fuel processing capability of the GDL in this work can result in major part of methane conversion occurring in the GDL than over the anode.

The above results indicate that there is a synergy between the rates of reactions in the GDL and over the anode. In the setup of SOFC plus GDL, the major reaction process is:

(1) In the GDL, the incoming methane encounters CO_2 coming from the anode to perform CO_2 reforming of methane. This produces CO in the GDL.
(2) The transport of the produced CO and the remaining methane to the anode to produce CO_2 and CO.

Therefore, an increased rate of CO formation in the GDL can lead to an increased rate of CO_2 formation over the anode, which then increases the rate of CO_2 reforming of methane in the GDL. Notably, H_2 is transported to and also produced over the anode. However, as discussed in the above, H_2 cannot compete with either methane or CO to be adsorbed over the anode and thus the amount of possible H_2O formation is zero or too small to be detectable.

Fig. 6 shows similar CO and CO_2 behaviors as those of Fig. 5. This confirms the above-described reactions in the GDL and over the anode. However, the region where the rate of CO formation is larger than that of CO_2 formation becomes smaller with this increase of the CH_4 concentration from 30 to 50%. This is attributed to that the concentration of the C species increases with increasing
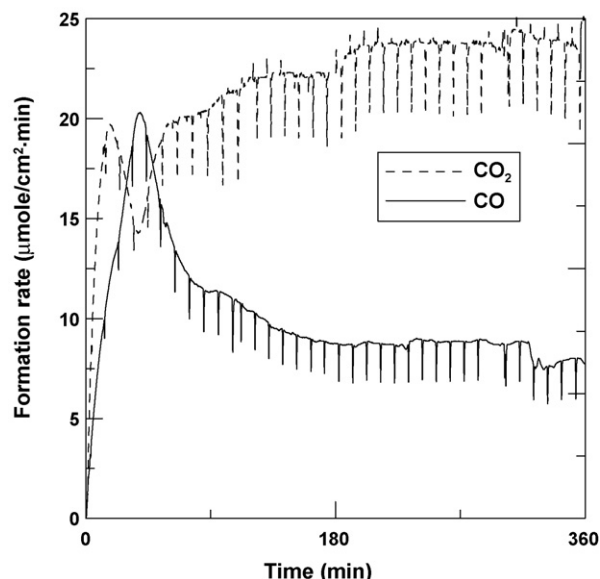

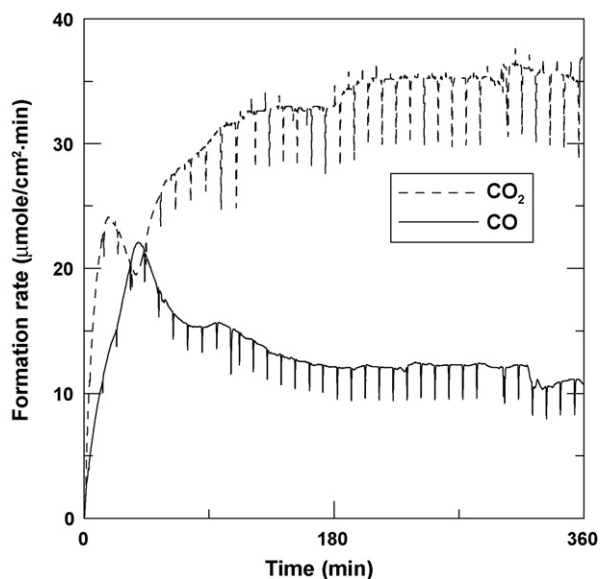**Fig. 6.** Profiles of CO and CO_2 formation rates with 50% CH_4 as the fuel.

Fig. 7. Profiles of CO and CO_2 formation rates with 70% CH_4 as the fuel.

CH_4 concentration and thus the net rate of CO_2 formation increases according to the above discussion, which is based on CO_2 reforming of methane being the major reaction in the GDL. This is in accordance with an increasing CO_2 selectivity with increasing methane concentration, as shown in Table 1. This also explains the observation that, when the initial period of carbon deposition shifts to that of de-coking, the formation rate of CO_2 increases from its minimum while that of CO decreases from its maximum. Notably, according to the above discussion, de-coking is a reaction step in the overall reaction of CO_2 reforming of methane; the activity of this reaction is enhanced by the impregnated GDC due to its high content of mobile lattice oxygen and high oxygen-ion conductivity.

Fig. 7 shows similar CO and CO_2 behaviors as those of Figs. 5 and 6. This again confirms the above-described reactions in the GDL and over the anode. Also, the region where the rate of CO formation is larger than that of CO_2 formation becomes even smaller with this increase of the CH_4 concentration from 50 to 70%. This is again in accordance with the CO_2 reforming of methane being the major reaction in the GDL. Additionally, Table 1 also shows that, as the methane concentration increases, the increased amount of CO_2 formation is much larger than that of CO formation. This is attributed to that larger methane concentration results in larger amount of deposited C species, which results in larger rate of CO_2 reforming of methane in the GDL.

DM-SOFCs with fuel-processing GDL can have surface modifications of the GDLs with other catalytic materials to improve the SOFC performance. According to the results of this work, a catalytic material with a higher activity for CO_2 reforming of methane may

be expected to result in a better fuel-processing activity of GDL and thus an improved the DM-SOFC performance.

4. Conclusions

(1) In the setup of SOFC plus GDL, the current density, the methane conversion rate, the product formation rates, and the CO_2 selectivity increased with increasing methane concentration.
(2) There is no H_2O formation either over the anode or in the GDL, indicating the inertness of the SOFC towards H_2 conversion during direct-methane reaction.
(3) The major reaction in the GDL is CO_2 reforming of methane to produce the syngas. The activity of this reaction is enhanced by the impregnated GDC.
(4) The anodic electrochemical oxidation of CO from GDL enhances the SOFC performance in terms of the current density, in comparison to SOFCs without GDL.
(5) There is a synergy between the rate of CO_2 reforming of methane in the GDL and that of electrochemical oxidation of CO over the anode.

References

[1] P. Aguiar, C.S. Adjiman, N.P. Brandon, J. Power Sources 138 (2004) 120.
[2] N. Laosiripojana, S. Assabumrungrat, J. Power Sources 163 (2007) 943.
[3] V.M. Janardhanan, V. Heuveline, O. Deutschmann, J. Power Sources 172 (2007) 296.
[4] Y. Lin, Z. Zhan, S.A. Barnett, J. Power Sources 158 (2006) 1313.
[5] Y. Yin, S. Li, C. Xia, G. Meng, J. Power Sources 167 (2007) 90.
[6] J.B. Wang, J.C. Jang, T.J. Huang, J. Power Sources 122 (2003) 122.
[7] Y. Lin, Z. Zhan, J. Liu, S.A. Barnett, Solid state Ionics 176 (2005) 1827.
[8] C. Mallon, K. Kendall, J. Power Sources 145 (2005) 154.
[9] M. Ihara, K. Matsuda, H. Sato, C. Yokoyama, Solid state Ionics 175 (2004) 51.
[10] T.J. Huang, M.C. Huang, J. Power Sources 168 (2007) 229.
[11] W.Z. Zhu, S.C. Deevi, Mater. Sci. Eng. A 348 (2003) 227.
[12] T.J. Huang, M.C. Huang, J. Power Sources 185 (2008) 1315.
[13] C. Finnerty, G.A. Tompsett, K. Kendall, R.M. Ormerod, J. Power Sources 86 (2000) 459.
[14] Z. Zhan, S.A. Barnett, Science 308 (2005) 844.
[15] C. Sun, Z. Xie, C. Xia, H. Li, L. Chen, Electrochem. Commun. 8 (2006) 833.
[16] X.F. Ye, S.R. Wang, Z.R. Wang, L. Xiong, X.F. Sun, T.L. Wen, J. Power Sources 177 (2008) 419.
[17] W. Zhu, C. Xia, J. Fan, R. Peng, G. Meng, J. Power Sources 160 (2006) 897.
[18] M.C. Huang, T.J. Huang, J. Power Sources 191 (2009) 555.
[19] T.J. Huang, T.C. Yu, Catal. Lett. 102 (2005) 175.
[20] T.J. Huang, M.C. Huang, W.J. Chen, C.L. Chou, Oscillation of electrical current during direct methane oxidation over Ni-added LSCF-GDC anode of solid oxide fuel cells, Chem. Eng. J. (2009), doi:10.1016/j.cej.2009.06.014.
[21] T.J. Huang, C.L. Chou, M.C. Huang, W.J. Chen, Electrochem. Commun. 11 (2009) 294.
[22] T.J. Huang, M.C. Huang, Chem. Eng. J. 138 (2008) 538.
[23] T.J. Huang, M.C. Huang, J. Power Sources 175 (2008) 473.
[24] T.J. Huang, M.C. Huang, Chem. Eng. J. 135 (2008) 216.
[25] T.J. Huang, C.H. Wang, J. Power Sources 163 (2006) 309.
[26] T.J. Huang, C.H. Wang, Chem. Eng. J. 132 (2007) 97.
[27] T.J. Huang, C.H. Wang, Catal. Lett. 118 (2007) 103.
[28] T.J. Huang, M.C. Huang, Int. J. Hydrogen Energy 33 (2008) 5073.
[29] T.J. Huang, H.C. Lin, T.C. Yu, Catal. Lett. 105 (2005) 239.
[30] J.B. Wang, Y.S. Wu, T.J. Huang, Appl. Catal. A: Gen. 272 (2004) 289.
[31] T. Kim, S. Moon, S.I. Hong, Appl. Catal. A: Gen. 224 (2002) 111.